Vertical distributions of N_2O isotopocules in the equatorial stratosphere

Sakae Toyoda[1], Naohiro Yoshida[1,2], Shinji Morimoto[3], Shuji Aoki[3], Takakiyo Nakazawa[3], Satoshi Sugawara[4], Shigeyuki Ishidoya[5], Mitsuo Uematsu[6], Yoichi Inai[3], Fumio Hasebe[7], Chusaku Ikeda[8], Hideyuki Honda[8], Kentaro Ishijima[9]

[1] Department of Chemical Science and Engineering, School of Materials and Chemical Technology, Tokyo Institute of Technology, Yokohama 226-8502, Japan
[2] Earth-Life Science Institute, Tokyo Institute of Technology, Tokyo 152-8550, Japan
[3] Center for Atmospheric and Oceanic Studies, Graduate School of Science, Tohoku University, Sendai 980-8578, Japan
[4] Miyagi University of Education, Sendai 980-0845, Japan
[5] National Institute of Advanced Industrial Science and Technology (AIST), Tsukuba 305-8569, Japan
[6] Atmosphere and Ocean Research Institute (AORI), The University of Tokyo, Kashiwa, 277-8564, Japan
[7] Division of Earth System Science, Graduate School of Environmental Science, Hokkaido University, Sapporo 060-0810, Japan
[8] Institute of Space and Astronautical Sciences (ISAS), Japan Aerospace Exploration Agency (JAXA), Sagamihara 252-5210, Japan
[9] Project Team for HPC Advanced Predictions Using Big Data, Japan Agency for Marine-Earth Science and Technology (JAMSTEC), Yokohama, 236-0001, Japan

Correspondence to: Sakae Toyoda (toyoda.s.aa@m.titech.ac.jp)

Abstract. Vertical profiles of nitrous oxide (N_2O) and its isotopocules, isotopically substituted molecules, were obtained over the equator at altitudes of 16–30 km. Whole air samples were collected using newly developed balloon-borne compact cryogenic samplers over the Eastern Equatorial Pacific in 2012 and Biak Island, Indonesia in 2015. They were examined in the laboratory using gas chromatography and mass spectrometry. The mixing ratio and isotopocule ratios of N_2O in the equatorial stratosphere showed a weaker vertical gradient than the previously reported profiles in the subtropical and mid-latitude and high-latitude stratosphere. From the relation between the mixing ratio and isotopocule ratios, further distinct characteristics were found over the equator: (1) Observed isotopocule enrichment factors (ε values) in the middle stratosphere (25–30 km or $[N_2O]$ < ca. 260 nmol mol^{-1}) are almost equal to ε values reported from broadband photolysis experiments conducted in the laboratory. (2) ε values in the lower stratosphere (< ca. 25 km or $[N_2O]$ > ca. 260 nmol mol^{-1}) are about half of the experimentally obtained values, being slightly larger than those observed in the mid-latitude and high-latitude lower stratosphere ($[N_2O]$ > ca. 170 nmol mol^{-1}). These results suggest the following. (1) The time scale of horizontal mixing in the tropical middle stratosphere is sufficiently large for in-situ photolysis of N_2O, mainly because of strong upwelling and transport barrier between the tropics and extratropics. (2) The air in the tropical lower stratosphere is exchanged with

extratropical air on a time scale that is shorter than that of photochemical decomposition of N_2O. Previously observed ε values, which are invariably smaller than those of photolysis, can be explained qualitatively using a three-dimensional chemical transport model and using a simple model that assumes mixing of 'aged' tropical air and extratropical air during residual circulation. Results show that isotopocule ratios are useful to examine the stratospheric transport scheme deduced from tracer–tracer relations.

Keywords. nitrous oxide, stable isotopes, tropical stratosphere, cryogenic sampling, stratospheric transport, stratospheric photochemistry

1 Introduction

Nitrous oxide (N_2O) is a potent greenhouse gas and stratospheric ozone depleting substance emitted from various sources on the Earth surface. It is injected into the stratosphere in tropical upwelling regions. In the stratosphere, it is transported meridionally by so-called Brewer–Dobson circulation and is decomposed by photolysis (Eq. 1) and photooxidation (Eq. 2) with approximate shares of 90% and 10%, respectively (Minschwaner et al., 1993).

$$N_2O + h\nu \rightarrow N_2 + O(^1D) \quad (1)$$

$$N_2O + O(^1D) \rightarrow 2NO \quad (2a)$$

$$\rightarrow N_2 + O_2 \quad (2b)$$

Mixing ratios of trace gases such as N_2O and their interrelationships are regarded as useful tools to establish a detailed picture of stratospheric circulation (Plumb, 2007), and previous observations showed compact tracer relationships that depend on latitude (e.g, Michelsen et al., 1998). Natural abundance ratios of N_2O isotopocules, molecular species that only differ in either the number or position of isotopic substitutions (Coplen, 2011), are useful tracers for elucidating the sources and physicochemical records of N_2O because isotopocule ratios reflect the isotopic compositions of source materials, isotope effects specific to each chemical and physical process relevant to formation, transportation, and decomposition of N_2O, and mixing of various air and water masses (Toyoda et al., 2015). In the context of stratospheric distribution, isotopocule ratios are unique in their ability to provide the degree of photochemical decomposition and the relative importance of the above-mentioned two decomposition pathways (Toyoda et al., 2001; Röckmann et al., 2001).

Stratospheric distributions of N_2O isotopocules have been studied using scientific balloons and aircraft. For balloon observations, (a) whole air samples are collected using cryogenic samplers and are evaluated using isotope ratio monitoring mass spectrometry (IRMS) (Kim and Craig, 1993; Rahn and Wahlen, 1997; Röckmann et al., 2001; Toyoda et al., 2001; Toyoda et al., 2004; Kaiser et al., 2006); alternatively, (b) remote measurements are conducted using Fourier-transform infrared spectrometry (Griffith et al., 2000). Such observations have revealed vertical profiles up to 35 km altitude. For aircraft observations, whole air samples are collected using pressurizing pumps, with subsequent evaluation by IRMS (Rahn and Wahlen, 1997; Park et al., 2004; Kaiser et al., 2006). Although these observations are limited to ca. 20 km altitude, vertical profiles can be obtained for horizontally wide areas such as Arctic polar vortexes.

Earlier studies showed that a decrease in the mixing ratio of N_2O with altitude is accompanied by enrichment of isotopocules of N_2O heavier than the major one ($^{14}N^{14}N^{16}O$) (Kim and Craig, 1993; Rahn and Wahlen, 1997). The results were consistent with the expected isotopocule fractionation during photolysis (Yung and Miller, 1997), but the apparent degrees of fractionation (isotopocule enrichment factor, ε) differed between those of the lower (< 20–25 km where N_2O mixing ratio > 180-250 nmol mol^{-1}) and middle (> 20–25 km or < 180-250 nmol mol^{-1}) stratosphere (Toyoda et al., 2001; Röckmann et al., 2001; Kaiser et al., 2006; Park et al., 2004). They are always smaller than that obtained from laboratory photolysis experiments (Röckmann et al., 2000; Turatti et al., 2000; Zhang et al., 2000; Kaiser et al., 2002b; 2003) or absorption spectra (von Hessberg et al., 2004). Moreover, the values of ε for the middle stratosphere were found to depend on the latitude and season (Toyoda et al., 2004; Kaiser et al., 2006; Park et al., 2004). Such variation has been regarded as a result of photochemical and transport processes (McLinden et al., 2003; Park et al., 2004; Kaiser et al., 2006), but it has not been fully examined because of the lack of measurements taken over the tropicalupwelling regions. As noted above, tropical stratosphere is the starting point of meridional transportation of N_2O injected from the troposphere and the rates of photochemical reactions are faster than those in the extratropics because of stronger actinic flux. Although there are a few reports on vertical profiles of N_2O isotopocules over India (18°N) (Röckmann et al., 2001; Kaiser et al., 2006), isotopic composition of N_2O in upwelling tropical air has not been characterized.

Another controversial problem about the stratospheric N_2O is whether the photooxidation sink (Eq. 2) has larger contribution than 10% in the lower stratosphere. Kaiser and coworkers found that the ratios of enrichment factors of isotopocule during photolysis and photooxidation are distinct (Kaiser et al., 2002a) and they estimated that a much larger fraction than 10% is removed by photooxidation at least in the lower stratosphere (N_2O mixing raitos > 300 nmol mol^{-1}) (Kaiser et al., 2006). However, similar but a little

simplified analyses by Park et al. (2004) and Toyoda et al. (2004) could not detect significant differences in the enrichment factor ratios between the lower and middle stratospheres, and Park et al. (2004) speculated that the enrichment factor ratios could be affected not only by the relative share of the two sink pathways but also by other factors such as transport.

This study was conducted to ascertain the vertical profiles of N_2O and its isotopocules over the equator and to examine the factors that control the apparent isotopic fractionation in the stratosphere by comparing results from earlier studies and three-dimentional chemical transport model simulation.

2 Experiments and model simulation

2.1 Whole air sampling over the equator

Stratospheric air samples were collected using balloon-borne compact cryogenic samplers (J-T samplers) (Morimoto et al., 2009). The sampler consists of an evacuated 800 cm^3 stainless steel sample flask (SUS304), a cooling device called a Joule–Thomson (J-T) mini cooler, a two-liter high-pressure neon gas cylinder, pneumatic valves, solenoid valves, a 100 cm^3 high-pressure N_2 gas cylinder for actuation of pneumatic valves, an electronic controller with a GPS receiver, a telemetry transmitter, and batteries. The J-T mini cooler can produce liquid neon from high-pressure neon gas that is pre-cooled by liquid nitrogen. The liquid neon is used as refrigerant to solidify or liquefy the stratospheric air. Contrasted against the larger sampling system used in our previous observations, which was about 250 kg with 12 sample flasks in a Dewar flask filled with liquid helium, the J-T sampler is ca. 20 kg, with operational and logistic advantages at remote sites such as remote islands or polar regions.

Sampling over the eastern equatorial Pacific (0°N, 105°W–115°W) was conducted on February 4, 5, 7, and 8, 2012 during the KH-12-1 cruise of R/V Hakuho-maru, JAMSTEC as a part of the Equatorial Pacific Ocean and Stratospheric/tropospheric Atmosphere Study Program. For each balloon flight, a 5–8 L STP of air sample was collected by a single sampler at programmed altitude of 19–29 km. The sampler then descended by parachute. It was later recovered on the sea.

Another sampling campaign was conducted at Biak Island, Indonesia (1°S, 136°E) on February 22, 24, 26, and 28, 2015 as a part of Small-Size Project by ISAS / JAXA (Hasebe et al., submitted). For each balloon flight, two samplers integrated into a single gondola were launched from the observatory of National Institute

of Aeronautics and Space of the Republic of Indonesia (LAPAN). Samples were collected at two altitudes. Therefore, in total, we obtained seven samples: two samples on each of four flights, with one failed sampling.

Locations of launching sites are shown in Figure 1. Balloon trajectories are portrayed in Figure S2. Sampling was conducted while the balloon was ascending except the flight on Feb 5, 2012. Typical altitude range was about 2 km, and we took the central value of the range as the sampling altitude.

2.2 Analysis of mixing ratio and isotopocule ratios

At Tohoku University, the mixing ratio of N_2O was measured using gas chromatography with electron capture detection (GC-ECD) with precision of 1 nmol mol^{-1} (Ishijima et al., 2001). The isotopocule ratios, defined as follows, were measured at Tokyo Institute of Technology using gas chromatography – isotope ratio mass spectrometry (Toyoda et al., 2004; Toyoda and Yoshida, 2016).

$$\delta X = (R_{\text{sample}} - R_{\text{standard}}) / R_{\text{standard}}, \quad (3)$$

Therein, X denotes $^{15}N^{\alpha}$, $^{15}N^{\beta}$ or ^{18}O, and where R denotes $^{14}N^{15}N^{16}O/^{14}N^{14}N^{16}O$, $^{15}N^{14}N^{16}O/^{14}N^{14}N^{16}O$ or $^{14}N^{14}N^{18}O/^{14}N^{14}N^{16}O$ of the sample and standards (Toyoda and Yoshida, 1999). The δ value is expressed as the permil (‰) deviation relative to atmospheric N_2, and Vienna Standard Mean Ocean Water (VSMOW), respectively, for nitrogen and oxygen. In addition to $\delta^{15}N^{\alpha}$ and $\delta^{15}N^{\beta}$, the δ value for bulk N and ^{15}N-site preference (SP) are often used as illustrative parameters:

$$\delta^{15}N^{\text{bulk}} = (\delta^{15}N^{\alpha} + \delta^{15}N^{\beta}) / 2 \quad (4)$$

$$SP = \delta^{15}N^{\alpha} - \delta^{15}N^{\beta}. \quad (5)$$

Duplicate analyses were made for a set of two runs: monitoring of molecular ion for determination of $\delta^{15}N^{\text{bulk}}$ and $\delta^{18}O$ and NO^+ fragment ion for determination of $\delta^{15}N^{\alpha}$. A 300–400 cm^3 STP aliquot of the sample air was introduced into the analytical system from the sample flask in a single run. Typical precisions of the isotopic analyses are < 0.1‰ for $\delta^{15}N^{\text{bulk}}$, < 0.2‰ for $\delta^{18}O$, and < 0.5‰ for $\delta^{15}N^{\alpha}$, although they were slightly worse for samples collected at higher altitudes because of the lower N_2O mixing ratio.

To analyze the relation between the N_2O mixing ratio ($[N_2O]$) and isotopocule ratio (δ) in a Rayleigh fractionation scheme (Eq. 6), measured values must be normalized with respect to the values before the air mass enters the stratosphere.

$$(1+\delta)/(1+\delta_0) = \{[N_2O]/[N_2O]_0\}^{\varepsilon} \quad (6)$$

In Eq. 6, subscript 0 signifies a tropospheric value; ε is the enrichment factor. Because the tropospheric mixing ratio and isotopocule ratios are known to have secular trends, $[N_2O]_0$ and δ_0 were estimated as follows. First, the age of the measured air mass was estimated based on the mixing ratio of CO_2, which was also measured for the same air sample (Engel et al., 2009). Then, the N_2O mixing ratio at the time when the air mass was in the troposphere was calculated using the estimated age of air and the secular trend of tropospheric mixing ratio observed by the ALE/GAGE/AGAGE project (Prinn et al., 2000). We used AGAGE data from Mace Head (Ireland) to calculate $[N_2O]_0$ for stratospheric air in the tropics (this study) and the Northern Hemisphere (in which our previous observations were conducted) and those from Cape Grim (Tasmania) for the Southern Hemisphere (our previous observation in Antarctica). For calculating δ_0, the secular trends observed at Hateruma island, Japan (Toyoda et al., 2013) and Cape Grim (Park et al., 2012) were used, respectively, for the tropics/Northern Hemisphere and the Southern Hemisphere. In Table S3 we compare how much this correction regarding the age of air changed the position of each data point in Figs. 3 and 5. Typically, the term related to mixing ratio ($-\ln\{[N_2O]/[N_2O]_{trp}\}$) is decreased by 0.2–3% when we use $[N_2O]_0$, the value when the air mass actually entered into the stratosphere, instead of the value at the same time of the observation, $[N_2O]_{trp}$. The isotopic terms ($\ln\{(1+\delta)/(1+\delta_{trp})\}$) are either increased or decreased depending on their secular trends, and they are changed by 0.2–3%.

2.3 Simulation using a three-dimensional chemical transport model

To examine the factors controlling the stratospheric distributions of N_2O isotopocules, a numerical simulation was conducted using the Center for Climate System Research/National Institute for Environmental Studies/Frontier Research Center for Global Change atmospheric general circulation model with chemical reactions (CCSR/NIES/FRCGC ACTM) (Ishijima et al., 2010; Ishijima et al., 2015). Because Ishijima et al. (2015) have already given a detailed description of the N_2O isotopocule model, we briefly explain it here.

The N_2O photolysis rate was calculated for 15 bins from 178 to 200 nm and for 3 bins from 200 to 278 nm using a scheme incorporating the parameterization of Minschwaner et al. (1993) (Akiyoshi et al., 2009) and by a main radiation – photolysis scheme of the ACTM (Sekiguchi and Nakajima, 2008). Fractionation of N_2O isotopocules was simulated using wavelength-dependent and temperature-dependent enrichment factors (ε) for $^{14}N^{15}N^{16}O$ and $^{15}N^{14}N^{16}O$ reported by von Hessberg et al. (2004) although the ε for $^{14}N^{14}N^{18}O$ was estimated from the relation between apparent ε for each isotopocule observed in the stratosphere due to the lack of suitable experimental reports. The model transport was nudged to ERA-interim reanalysis (Dee et al., 2011) for horizontal winds and temperature at 6-hourly time intervals. Regarding the photooxidation sink of

N_2O, the concentration of $O(^1D)$ was calculated online in the ACTM; ε values were calculated as described by Kaiser et al. (2002a).

While both the surface emissions and the photolytic isotopocule fractionations were optimized in the earlier work by Ishijima et al. (2015), only the former was optimized in the present study. This is because we considered that it would be better to keep the experimentally determined original isotopocule enrichment factors for the purpose of comparison between the model and the observations in the stratosphere. Moreover, we found that apparent isotopocule enrichment factors obtained by the model simulation become much closer to those by the balloon observations by replacing the meteorological data from JRA-25 (Onogi et al., 2007) with those from ERA-interim. This is probably because dynamics and chemical reactions in the model was improved by the replacement of the meteorological reanalysis data for nudging. Surface emissions of the four N_2O isotopocules were optimized in the manner described in an earlier report (Ishijima et al., 2015), with emissions modified to reproduce observed trends (Röckmann and Levin, 2005) and interhemispheric differences (Ishijima et al., 2007) of atmospheric N_2O isotopocule mixing ratios. Consequently, the estimated emissions were used for a forward simulation of four N_2O isotopocules in the atmosphere from the surface to the stratosphere in this study. The emissions and tropospheric values are reasonable (see Supplemental Information) compared to those of past studies (e.g., Toyoda et al., 2013; Toyoda et al., 2015) in terms of the necessary order of precision for analysis of the large vertical profiles in the stratosphere in this study.

3 Results and discussion

3.1 Vertical profiles of the N_2O mixing ratio and isotopocule ratios over the Equator

In all, 11 samples (4 from the eastern Pacific, 7 at Biak Island) were collected at target altitudes; of them, 10 were measured for N_2O isotopocules. Figure 2 presents vertical profiles of the N_2O mixing ratio, $\delta^{15}N^{bulk}$, SP, and $\delta^{18}O$ observed over the equator. Data from our previous observations over Japan, Sweden, and Antarctica and those from observations by Röckmann et al. (2000) and Kaiser et al. (2006) conducted over India are also shown. The height of the tropical tropopause layer (TTL) was 14–18.5 km (Fueglistaler et al., 2009), whereas the tropopause height was 12–16 km over Japan and 9 or 10 km over Sweden and Antarctica (Table S1). As observed at mid-latitudes and high latitudes, the mixing ratio decreases with height; isotopocule ratios increase with height over the equator. However, the vertical gradient is weaker at lower latitudes. Our observation over the equator shows the weakest gradient. Although a slight difference in mixing ratio was observed for 20–25 km, the two equatorial profiles obtained at different longitudes over the equator agreed quite well. We combined the two datasets as a single one for further examinations.

3.2 Correlation between mixing ratio and isotopocule ratios: apparent isotopocule enrichment factors

In Fig. 3 and Figs. S3–S5, the isotopocule ratios are shown against the N_2O mixing ratio after the normalization described in Eq. 6 (Rayleigh plot). The equatorial data for lower altitudes ($-\ln\{[N_2O]/[N_2O]_0\}$ < 0.2 or $[N_2O]$ > ca. 260 nmol mol^{-1}) are on the line defined by the data for lower altitudes ($-\ln\{[N_2O]/[N_2O]_0\}$ < 0.6 or $[N_2O]$ > 170 nmol mol^{-1}) over middle latitudes and high latitudes. The linear relation is consistent with isotopocule fractionation during the decomposition of N_2O in a closed system, although the slope of the line, which corresponds to isotopic enrichment factor (ε), is markedly lower than that obtained by laboratory photolysis experiments (see below). However, the three data points obtained at altitudes corresponding to $-\ln\{[N_2O]/[N_2O]_0\}$ > 0.2 ($[N_2O]$ < ca. 260 nmol mol^{-1}) show systematic deviation from the line and seem to define another line (Fig. 3b). A similar deviation or *bending* structure of the Rayleigh plot has also been observed at middle to high latitudes (Fig. 3a, from the points where the *x* axis value is ca. 0.5) (Toyoda et al., 2004). We therefore compare the slope of the lines obtained for observations at various latitudes and for laboratory simulation experiments.

As portrayed in Fig. 4, absolute values of ε ($|\varepsilon|$) for $^{15}N^{bulk}$, $^{15}N^{\alpha}$, and ^{18}O in the equatorial lower stratosphere are slightly higher than those of middle latitude and high latitude lower stratosphere, but they are still only about half of the ε obtained by broadband photolysis experiments (Kaiser et al., 2002b; Kaiser et al., 2003). In contrast, $|\varepsilon|$ in the higher region (or middle stratosphere) show larger values. They are the largest over the equator except for $\varepsilon(^{18}O)$. The equatorial values of ε almost coincide with those of photolysis. It is also noteworthy that $|\varepsilon|$ in the middle stratosphere in the arctic polar vortex (Sweden) is as small as that in the lower stratosphere and that latitudinal and year-to-year or seasonal variation are slight compared to those of the middle stratosphere in the lower stratosphere. Although the similar latitudinal and altitudinal dependence of ε has been reported previously for the latitudes ranging from 18°N to 89°N (Park et al., 2004; Kaiser et al., 2006), our equatorial data showed that the change in ε at altitude with higher N_2O mixing ratio and the ε value is exactly what would be expected during the N_2O photolysis.

3.3 Cause of the variation of stratospheric ε

We then discuss causes of (1) lower $|\varepsilon|$ value in the lower stratosphere, (2) increase of $|\varepsilon|$ in the middle stratosphere, and (3) the largest $|\varepsilon|$ in the equatorial middle stratosphere based on two factors: photochemical and transport processes.

3.3.1 Photochemical processes

During photochemical decomposition of N_2O, ε reportedly depends on the wavelength that photolyzes N_2O, the relative share of photolysis and photooxidation pathways (Eqs. 1 and 2), and temperature (Toyoda et al., 2004; Kaiser et al., 2006). Moreover, because of transport processes the stratosphere cannot be always treated as an isolated system which is a prerequisite for Rayleigh fractionation model. The ratio of ε values for independent isotopocules (e.g., $\varepsilon(^{15}N^{bulk})/\varepsilon(^{18}O)$), however, has been identified as a useful parameter to distinguish photolysis and photooxidation (Kaiser et al., 2002a) because its sensitivity to wavelength and temperature is small and it is not affected by mixing process. Figure 5 shows the data obtained in this study and some previous ones in δ–δ space after the normalization described in Eq. 6. Especially in Fig. 5b, almost all data show a compact linear relation without bending or curved structure apparent in the Rayleigh diagram. The slope, which corresponds to the ratio of ε values, is very close to the one expected for photolysis. This confirms that photochemical decomposition of N_2O is mainly caused by photolysis (Minshwaner et al., 1993), although the small fluctuation in the lower left region in Fig. 5a will be discussed later.

3.3.2 Transport processes

Transport processes accompanied by mixing of variously aged stratospheric air has been considered as the major cause of lower $|\varepsilon|$ value in the stratosphere than in the laboratory photochemical decomposition (Park et al., 2004; Kaiser et al., 2006). Our new observation revealed that all the N_2O isotopocules are fractionated by the almost ideal Rayleigh process in the middle stratosphere over the deep tropics where the stratosphere is effectively the most isolated relative to all other regions. This underlines how much transport and mixing affect the apparent ε value.

We then consider the effect of transport on the apparent ε at different latitudes with a conceptual two-dimensional circulation model in the tropical and extra-tropical stratosphere that was proposed to explain tracer–tracer correlation (Plumb, 2002). In the tropics, N_2O is decomposed gradually during upwelling of the air mass injected from the troposphere. The uppermost tropical air mass X_0 is then transported to middle latitudes and higher latitudes, where it begins downwelling. Because the vertical ascent rate in the tropics is much faster than quasi-horizontal transport, there is an apparent transport barrier between the tropics and extratropics (Plumb, 2007). Nevertheless, entrainment of air mass Y_i across the subtropical edge separating the two regions must occur to compensate mass flux in the lower region (Fig. 6).

If we assume tropical profiles of N_2O and its isotopocule ratios (e.g., $\delta^{15}N^{bulk}$) are determined purely by photochemistry with initial mixing ratio of 320 ppb, a delta value of 0‰ and a ε_{sink} of −50‰, then tropical air masses vertically divided from Y_8 through Y_1 and X_0 are expected to line up on a solid line as portrayed in Fig. 7. Next, let us consider that air mass X_0 is mixed with Y_1 to form X_1. Based on the mass balance of isotopocules before and after mixing, the resulting composition of X_1 is obtained as a curve, as shown in red in Fig. 7. Assuming arbitrarily that the mixing ratio of Y_1 to X_1 is 0.1, and repeating such mixing stepwise, then we obtain mixing ratio and isotope ratios of N_2O in X_1 through X_8 as black stars in Fig. 6. This hypothetical, continuous mixing produces a curve that is qualitatively consistent with observations made over the mid-latitudes or high latitudes.

The mixing effect must also be the cause of smaller ε in the equatorial lower stratosphere (Fig. 4). The mean age of air deduced from CO_2 mixing ratio is known to be significantly larger than the phase lag of the water vapor mixing ratio, a so-called tape recorder signal, in the tropical stratosphere, which is explainable by mixing of old air from the extratropics into the tropics (Waugh and Hall, 2002). In addition, the difference in age between the equator and mid-latitude (over Japan) decreases concomitantly with decreasing altitude (Sugawara et al., unpublished data), suggesting that the time scale of meridional mixing or transport is smaller in the lower stratosphere than in the middle stratosphere, as suggested by results of an earlier study (Boering et al., 1996).

3.3.3 Comparison with chemical transport model (ACTM) simulation

We further examined the importance of transport using ACTM. Figure 8 presents results of ACTM simulation with observational data. Although the model approximates the photolysis of N_2O in the longer wavelength region ($\lambda > 200$ nm) with lower spectral resolution, profiles of the N_2O mixing ratio and isotopocule ratios were reproduced well, except in the winter polar stratosphere, where dynamic processes specific to the polar vortex might not be simulated appropriately in the model. In Fig. 9, the model simulation and observations are compared on a Rayleigh plot. Again, the model reproduced the difference between tropical and mid-latitudes or high latitudes. Because in situ $\varepsilon_{photolysis}$ used in the model calculation is nearly the same between low and high latitudes (Fig. S6c), this agreement supports the inference that the major causes of the difference are transport and mixing, which was previously suggested by observations in the high latitudes (Park et al., 2004) and by 1D or 3D model studies (McLinden et al., 2003; Morgan et al., 2003).

3.4 Share of photolysis and photooxidation

Kaiser et al. (2006) used the ratio of ε values for $^{15}N^{bulk}$ and ^{18}O (ψ) and the ratio of ε values for $^{15}N^{\alpha}$ and $^{15}N^{\beta}$ (η) to estimate the relative share of photolysis and photooxidation based on the fact that ψ and η are almost independent of transport processes and are significantly different between the two decomposition processes. They computed ψ and η values directly for each individual sample in order to avoid statistical errors associated with linear regression to the δ–δ plot which was adopted by Toyoda et al. (2004) and Park et al. (2004). In Fig. 10, we show ψ and η values calculated using the data presented in Fig. 2 in the manner similar to that of Kaiser et al. (2006) except that we used individual date of stratospheric entry for each data to normalize the δ values instead of using a single tropopause date. Although it is noteworthy that errors in ψ and η values increase concomitantly with decreasing altitude because of the decrease in the δ values, low values are obtained near the TTL over the Equator just as they are at other latitudes. This result confirms the indication by Kaiser et al. (2006) that the photooxidation sink has a much larger fraction than 10% in the lower stratosphere. Although the loss rate of N_2O in the lower stratosphere is very slow and the majority of N_2O injected into the stratosphere is photolyzed in the middle stratosphere as noted by Park et al. (2004), the share of photooxidation in *in situ* total loss increases in the lower stratosphere (Fig. S6b). Therefore, there is a possibility of additional decomposition of remaining N_2O during the transport (which should be slower than that of the tropical upwelling) and the isotopic signature of $O(^1D)$ pathway could be imprinted, and the photochemically aged air mass must be transported into the lower stratosphere of the tropics and extratropics. However, Morgan et al. (2003) reported that inclusion of isotope fractionation for photooxidation into their 2D model does not make a significant contribution to overall fractionation in the stratosphere, and Park et al. (2004) discussed an alternative modelling approach with and without $O(^1D)$ sink to test the importance of $O(^1D)$ reaction. Further studies using 3D model would be necessary to solve this controversial problem.

4 Conclusions

Vertical profiles of isotopocule ratios of N_2O in the equatorial stratosphere are found using balloon-borne compact cryogenic samplers and mass spectrometry in the laboratory. This report of the relevant literature is the first describing observations of them over the equator. Unlike other region of the stratosphere, enrichment factors for isotopocules in the middle equatorial stratosphere (25–30 km, or $[N_2O] < 260$ nmol mol^{-1}) agreed with those obtained with laboratory photolysis experiments, suggesting that the isotopocule ratios are determined mainly by photolysis because of weak vertical or horizontal mixing in the tropical upwelling. In the lower equatorial stratosphere (< ca. 25 km or $[N_2O] > 260$ nmol mol^{-1}), isotopocule ratios suggest that differently aged air masses are mixed because of the meridional transport and that decomposition by

photooxidation might also plays a significant role. Vertical and latitudinal distributions of N_2O and its isotopocules are found to be a unique tool to diagnose the relationship between photochemistry and transport in the stratosphere. Further observations of temporal variations and comparison with ACTM simulation will be needed to examine the change in the meridional circulation and obtain the quantitative estimate of the importance of photooxidation pathway.

Competing interests. The authors declare that they have no conflict of interest.

Acknowledgments. We thank researchers and crew of R/V Hakuho-maru KH-12-1 cruise for sampling over the eastern equatorial Pacific, and researchers and technical staff of LAPAN for the sampling over Biak. This work was supported by JSPS KAKENHI Grant Numbers 23224013 and 26220101 and also by JAXA as its Small-Size Project.

References

Akiyoshi, H., Zhou, L. B., Yamashita, Y., Sakamoto, K., Yoshiki, M., Nagashima, T., Takahashi, M., Kurokawa, J., Takigawa, M., and Imamura, T.: A CCM simulation of the breakup of the Antarctic polar vortex in the years 1980–2004 under the CCMVal scenarios, J. Geophys. Res., 114, D03103, doi: 10.1029/2007JD009261, 2009.

Boering, K. A., Wofsy, S. C., Daube, B. C., Schneider, H. R., Loewenstein, M., Podolske, J. R., and Conway, T. J.: Stratospheric mean ages and transport rates from observations of carbon dioxide and nitrous oxide, Science, 274, 1340-1343, 1996.

Coplen, T. B.: Guidelines and recommended terms for expression of stable-isotope-ratio and gas-ratio measurement results, Rapid Commun. Mass Spectrom., 25, 2538-2560, doi: 10.1002/rcm.5129, 2011.

Dee, D. P., Uppala, S. M., Simmons, A. J., Berrisford, P., Poli, P., Kobayashi, S., Andrae, U., Balmaseda, M. A., Balsamo, G., Bauer, P., Bechtold, P., Beljaars, A. C. M., van de Berg, L., Bid-lot, J., Bormann, N., Delsol, C., Dragani, R., Fuentes, M., Geer, A. J., Haimberger, L., Healy, S. B., Hersbach, H., Holm, E. V., Isaksen, L., Kallberg, P., Kohler, M., Matricardi, M., McNally, A. P., Monge-Sanz, B. M., Morcrette, J.-J., Park, B.-K., Peubey, C., de Rosnay, P., Tavolato, C., Thepaut, J.-N., and Vitart, F.: The ERA-Interim reanalysis: Configuration and performance of the data assimilation system, Q. J. Roy. Meteor. Soc., 137, 553-597, doi: 10.1002/qj.828, 2011.

Engel, A., Möbius, T., Bönisch, H., Schmidt, U., Heinz, R., Levin, I., Atlas, E., Aoki, S., Nakazawa, T., Sugawara, S., Moore, F., Hurst, D., Elkins, J., Schauffler, S., Andrews, A., and Boering, K.: Age of

stratospheric air unchanged within uncertainties over the past 30 years, Nat. Geosci., 2, 28-31, doi: 10.1038/ngeo388, 2009.

Fueglistaler, S., Dessler, A. E., Dunkerton, T. J., Folkins, I., Fu, Q., and Mote, P. W.: Tropical tropopause layer, Rev. Geophys., 47, RG1004, doi: 10.1029/2008RG000267, 2009.

Griffith, D. W. T., Toon, G. C., Sen, B., Blavier, J.-F., and Toth, R. A.: Vertical profiles of nitrous oxide isotopomer fractionation measured in the stratosphere, Geophys. Res. Lett., 27, 2485-2488, 2000.

Hasebe, F., Aoki, S., Morimoto, S., Inai, Y., Nakazawa, T., Sugawara, S., Ikeda, C., Honda, H., Yamazaki, H., Halimurrahman, Komala, N., Putri, F. A., Budiyono, A., Soedjarwo, M., Ishidoya, S., Toyoda, S., Shibata, T., Hayashi, M., Eguchi, N., Nishi, N., Fujiwara, M., Ogino, S.-Y., Shiotani, M., and Sugidachi, T.: Observations of dynamics and chemistry in the tropical upper atmosphere to disentangle the processes responsible for global circulation changes, submitted to B. Am. Meteorol. Soc.

Ishijima, K., Nakazawa, T., Sugawara, S., Aoki, S., and Saeki, T.: Concentration variations of tropospheric nitrous oxide over Japan, Geophys. Res. Lett., 28, 171-174, 2001.

Ishijima, K., Patra, P. K., Takigawa, M., Machida, T., Matsueda, H., Sawa, Y., Steele, L. P., Krummel, P. B., Langenfelds, R. L., Aoki, S., and Nakazawa, T.: Stratospheric influence on the seasonal cycle of nitrous oxide in the troposphere as deduced from aircraft observations and model simulations, J. Geophys. Res., 115, D20308, doi: 10.1029/2009JD013322, 2010.

Ishijima, K., Sugawara, S., Kawamura, K., Hashida, G., Morimoto, S., Murayama, S., Aoki, S., and Nakazawa, T.: Temporal variations of the atmospheric nitrous oxide concentration and its $\delta^{15}N$ and $\delta^{18}O$ for the latter half of the 20th century reconstructed from firn air analyses, J. Geophys. Res.: Atmos., 112, D03305, doi: 10.1029/2006/JD007208, 2007.

Ishijima, K., Takigawa, M., Sudo, K., Toyoda, S., Yoshida, N., Röckmann, T., Kaiser, J., Aoki, S., Morimoto, S., Sugawara, S., and Nakazawa, T.: Development of an atmospheric N_2O isotopocule model and optimization procedure, and application to source estimation, Atmos. Chem. Phys. Discuss., 15, 19947-20011, doi: 10.5194/acpd-15-19947-2015, 2015.

Kaiser, J., Brenninkmeijer, C. A. M., and Röckmann, T.: Intramolecular ^{15}N and ^{18}O fractionation in the reaction of N_2O with $O(^1D)$ and its implications for the stratospheric N_2O isotope signature, J. Geophys. Res., 107, ACH 16-11–ACH 16-14, doi: 10.1029/2001JD001506, 2002a.

Kaiser, J., Engel, A., Borchers, R., and Röckmann, T.: Probing stratospheric transport and chemistry with new balloon and aircraft observations of the meridional and vertical N_2O isotope distribution, Atmos. Chem. Phys., 6, 3535-3556, 2006.

Kaiser, J., Röckmann, T., and Brenninkmeijer, C. A. M.: Temperature dependence of isotope fractionation in N_2O photolysis, Phys. Chem. Chem. Phys., 4(18), 4420-4430, 2002b.

Kaiser, J., Röckmann, T., Brenninkmeijer, C. A. M., and Crutzen, P. J.: Wavelength dependence of isotope fractionation in N_2O photolysis, Atmos. Chem. Phys., 3, 303-313, 2003.

Kim, K.-R., and Craig, H.: Nitrogen-15 and oxygen-18 characteristics of nitrous oxide: A global perspective, Science, 262, 1855-1857, 1993.

McLinden, C. A., Prather, M. J., and Johnson, M. S.: Global modeling of the isotopic analogues of N_2O: Stratospheric distributions, budgets, and the ^{17}O - ^{18}O mass-independent anomaly, J. Geophys. Res., 108, 4233-4247, doi: 10.1029/2002JD002560, 2003.

Michelsen, H. A., Manney, G. L., Gunson, M. R., Zander, R.: Correlations of stratospheric abundances of NO_y, O_3, N_2O, and CH_4 derived from ATMOS measurements, J. Geophys. Res., 103, 28347-28359, 1998.

Minschwaner, K., Salawitch, R. J., and McElroy, M. B.: Absorption of solar radiation by O_2: implications for O_3 and lifetimes of N_2O, $CFCl_3$, and CF_2Cl_2, J. Geophys. Res., 98, 10543-10561, 1993.

Morgan, C. G., Allen, M., Liang, M. C., Shia, R. L., Blake, G. A., and Yung, Y. L.: Isotopic fractionation of nitrous oxide in the stratosphere: Comparison between model and observations, J. Geophys. Res.: Atmos., 109, doi: 10.1029/2003JD003402, 2004.

Morimoto, S., Yamanouchi, T., Honda, H., Aoki, S., Nakazawa, T., Sugawara, S., Ishidoya, S., Iijima, I., and Yoshida, T.: A new compact cryogenic air sampler and its application in stratospheric greenhouse gas observation at Syowa Station, Antarctica, J. Atmos. Ocean. Tech., 26, 2182-2191, 2009.

Onogi, K., Tsutsui, J., Koide, H., Sakamoto, M., Kobayashi, S., Hatsushika, H. Matsumoto, T., Yamazaki, N., Kamahori, H., Takahashi, K., Kadokura, S., Wada, K., Kato, K., Oyama, R.,Ose, T., Mannoji, N., and Taira, R.: The JRA-25 reanalysis, J. Meteorol. Soc. Jpn., 85, 369-432, 2007.

Park, S., Atlas, E. L., and Boering, K. A.: Measurements of N_2O isotopologues in the stratosphere: Influence of transport on the apparent enrichment factors and the isotopologue fluxes to the troposphere, J. Geophys. Res., 109, D01305, doi: 10.1029/2003JD003731, 2004.

Park, S., Croteau, P., Boering, K., Etheridge, D. M., Ferretti, D. F., Fraser, P. J., Kim, K.-R., Krummel, P. B., Langenfelds, R. L., Van Ommen, T. D., Steele, L. P., and Trudinger, C. M.: Trends and seasonal cycles in the isotopic composition of nitrous oxide since 1940, Nat. Geosci., 5, 261-265, doi: 10.1038/ngeo1421, 2012.

Plumb, R. A.: Stratospheric Transport, Journal of the Meteorological Society of Japan, 80, 793-809, 2002.

Plumb, R. A.: Tracer interrelationships in the troposphere, Rev. Geophys., 45, RG4005, doi: 10.1029/2005RG000179, 2007.

Prinn, R. G., Weiss, R. F., Fraser, P. J., Simmonds, P. G., Cunnold, D. M., Alyea, F. N., O'Doherty, S., Salameh, P., Miller, B. R., Huang, J., Wang, R. H. J., Hartley, D. E., Harth, C., Steele, L. P., Sturrock, G., Midgley, P. M., and McCulloch, A.: A History of Chemically and Radiatively Important Gases in Air deduced from ALE/GAGE/AGAGE, J. Geophys. Res., 105, 17,751-717,792, 2000.

Rahn, T., and Wahlen, M.: Stable Isotope Enrichment in Stratospheric Nitrous Oxide, Science, 278, 1776-1778, 1997.

Röckmann, T., Brenninkmeijer, C. A. M., Wollenhaupt, M., Crowley, J. N., and Crutzen, P. J.: Measurement of the isotope fractionation of $^{15}N^{14}N^{16}O$, $^{14}N^{15}N^{16}O$ and $^{14}N^{14}N^{18}O$ in the UV photolysis of nitrous oxide, Geophys. Res. Lett., 27, 1399-1402, 2000.

Röckmann, T., Kaiser, J., Brenninkmeijer, C. A. M., Crowley, J. N., R, Borchers, Br, W. A., and Crutzen, P. J.: Isotopic enrichment of nitrous oxide ($^{15}N^{14}NO$, $^{14}N^{15}NO$, $^{14}N^{14}N^{18}O$) in the stratosphere and in the laboratory, J. Geophys. Res., 106, 10403-10410, 2001.

Röckmann, T., and Levin, I.: High-precision determination of the changing isotopic composition of atmospheric N_2O from 1990 to 2002, J. Geophys. Res., 110, D21304, doi: doi:10.1029/2005JD006066, 2005.

Sekiguchi, M., and Nakajima, T.: A k-distribution-based radiation code and its computational optimization for an atmospheric general circulation model, Journal of Quantitative Spectroscopy & Radiative Transfer, 109, 2779-2793, 2008.

Toyoda, S., Kuroki, N., Yoshida, N., Ishijima, K., Tohjima, Y., and Machida, T.: Decadal time series of tropospheric abundance of N_2O isotopomers and isotopologues in the Northern Hemisphere obtained by using the long-term observation at Hateruma Island, Japan, J. Geophys. Res., 118, 3369-3381, doi: 10.1002/jgrd.50221, 2013.

Toyoda, S., and Yoshida, N.: Determination of nitrogen isotopomers of nitrous oxide on a modified isotope ratio mass spectrometer, Anal. Chem., 71, 4711-4718, 1999.

Toyoda, S., and Yoshida, N.: Development of automated preparation system for isotopocule analysis of N_2O in various air samples, Atmos. Meas. Tech., 9, 2093-2101, doi: 10.5194/amt-9-2093-2016, 2016.

Toyoda, S., Yoshida, N., Urabe, T., Aoki, S., Nakazawa, T., Sugawara, S., and Honda, H.: Fractionation of N_2O isotopomers in the stratosphere, J. Geophys. Res., 106, 7515-7522, 2001.

Toyoda, S., Yoshida, N., and Koba, K.: Isotopocule analysis of biologically produced nitrous oxide in various environments, Mass Spectrom. Rev., doi: 10.1002/mas.21459, 2015.

Toyoda, S., Yoshida, N., Urabe, T., Nakayama, Y., Suzuki, T., Tsuji, K., Shibuya, K., Aoki, S., Nakazawa, T., Ishidoya, S., Ishijima, K., Sugawara, S., Machida, T., Hashida, G., Morimoto, S., and Honda, H.:

Temporal and latitudinal distributions of stratospheric N_2O isotopomers, J. Geophys. Res., 109, D08308, doi: 10.1029/2003JD004316, 2004.

Turatti, F., Griffith, D. W. T., Wilson, S. R., Esler, M. B., Rahn, T., Zhang, H., and Blake, G. A.: Positionally dependent 15N fractionation factors in the UV photolysis of N_2O determined by high resolution FTIR spectroscopy, Geophys. Res. Lett., 27, 2489-2492, 2000.

von Hessberg, P., Kaiser, J., Enghoff, M. B., McLinden, C. A., Sorensen, S. L., Röckmann, T., and Johnson, M. S.: Ultra-violet absorption cross sections of isotopically substituted nitrous oxide species: $^{14}N^{14}NO$, $^{15}N^{14}NO$, $^{14}N^{15}NO$ and $^{15}N^{15}NO$, Atmos. Chem. Phys., 4, 1237-1253, 2004.

Waugh, D. W., and Hall, T. M.: Age of stratospheric air: Theory, observations, and models, Rev. Geophys., 40, 1010, doi: 10.1029/2000RG000101, 2002.

Yung, Y. L., and Miller, C. E.: Isotopic fractionation of stratospheric nitrous oxide, Science, 278, 1778-1780, 1997.

Zhang, H., Wennberg, P. O., Wu, V. H., and Blake, G. A.: Fractionation of $^{14}N^{15}N^{16}O$ and $^{15}N^{14}N^{16}O$ during photolysis at 213 nm, Geophys. Res. Lett., 27, 2481-2484, 2000.

Figure captions

Figure 1: Map showing balloon launching sites.

Figure 2: Vertical profiles of mixing ratio (a), $\delta^{15}N^{bulk}$ (b), *SP* (c), and $\delta^{18}O$ (d), of N_2O observed over the equator (pink symbols). Previously published results obtained over Japan (black and red symbols), Sweden (blue), and Antarctica (green) (Toyoda et al., 2001; 2004), and India (orange, Kaiser et al., 2016; Röckmann et al. 2001) are also shown. In the legend, launch sites and dates are shown, respectively, by three characters and six digits in yymmdd format. SBC, Sanriku Balloon Center, Japan; ESR, Esrange, Kiruna, Sweden; SYO, Syowa station, Antarctica; HDB, Hyderabad, India; EQP, Eastern equatorial Pacific; BIK, Biak island, Indonesia. See also Table S2 for details.

Figure 3: Correlation between mixing ratio and $\delta^{15}N^{bulk}$ of N_2O (Rayleigh plot). The high mixing ratio range (> ca. 120 nmol mol^{-1}) in (a) is enlarged in (b). Both parameters are normalized to their values at the time when the corresponding air mass entered the stratosphere (see Eq. 6 in the text). Grey solid and broken lines show slopes obtained respectively from laboratory broadband photolysis experiments (Kaiser et al., 2002; 2003) and photooxidation experiments (Kaiser et al., 2002; Toyoda et al., 2004).

Figure 4: Comparison of absolute values of the isotopocule enrichment factor ($|\varepsilon|$) for $^{15}N^{bulk}$, $^{15}N^{\alpha}$, and ^{18}O of N_2O between observations and laboratory experiments. L and M respectively refer to the lower and middle stratosphere with boundary mixing ratio of about 170 nmol mol^{-1} ($-\ln\{[N_2O]/[N_2O]_0\} = 0.6$) and 260 nmol mol^{-1} ($-\ln\{[N_2O]/[N_2O]_0\} = 0.2$) for extratropics and tropics, respectively, based on the Rayleigh plot shape (Fig. 3). The respective $|\varepsilon|$ for Japan, Sweden, and Antarctica are from Toyoda et al. (2004). Those for photolysis and photooxidation experiments are referred from reports by Kaiser et al. (2002; 2003) and Toyoda et al. (2004). Error

bars show either the standard deviation for the mean value (observation over Japan and photooxidation experiments), standard error associated with linear regression in Rayleigh plot (observations except Japan), or the possible range for stratospheric conditions (photolysis experiments).

Figure 5: Correlations between $\delta^{15}N^{\beta}$ and $\delta^{15}N^{\alpha}$ of N_2O (a) and between $\delta^{18}O$ and $\delta^{15}N^{bulk}$ of N_2O (b). The δ values are normalized as noted in the text. Grey solid and broken lines show slopes obtained respectively from laboratory broadband photolysis experiments (Kaiser et al., 2002; 2003) and photooxidation experiments (Kaiser et al., 2002; Toyoda et al., 2004).

Figure 6: Conceptual two-dimensional circulation model to analyze mixing processes between tropics and extratropics (from Plumb, 2002). The X_0 is the uppermost tropical stratospheric air mass, X_i (i = 1–8) are air masses formed by mixing of X_{i-1} and Y_i.

Figure 7: Presentation of X_i (black stars) obtained using the mixing model with assumed Y_i in the Rayleigh plot. The straight line shows tropical vertical isotopocule fractionation without transport/mixing effect. Curves show mixing between X_{i-1} and Y_i where mixing ratio Y_i/X_i is assumed to be 0.1.

Figure 8: Comparison of vertical profiles of mixing ratio (a) and $\delta^{15}N^{bulk}$ (b) of N_2O between observations and simulation by the ACTM. Model simulations for equatorial profiles were conducted for two dates because the observations were conducted during a 5-day or 7-day period.

Figure 9: Comparison of results of ACTM simulation and stratospheric observation in Rayleigh plot. The square region shown by broken lines in panel (a) is enlarged in panel (b).

Figure 10: Vertical profiles of ratio of ε values for $^{15}N^{bulk}$ and ^{18}O (ψ) and the ratio of ε values for $^{15}N^{\alpha}$ and $^{15}N^{\beta}$ (η) calculated in the manner similar to that of Kaiser et al. (2006). Grey bands show values obtained by laboratory broadband photolysis experiments (Kaiser et al., 2002; 2003) and photooxidation experiments (Kaiser et al., 2002; Toyoda et al., 2004) with widths representing their uncertainty. For photolysis, uncertainties associated with temperature (190–240 K) and wavelength (190–220 nm) dependency are shown with dark and light gray, respectively.

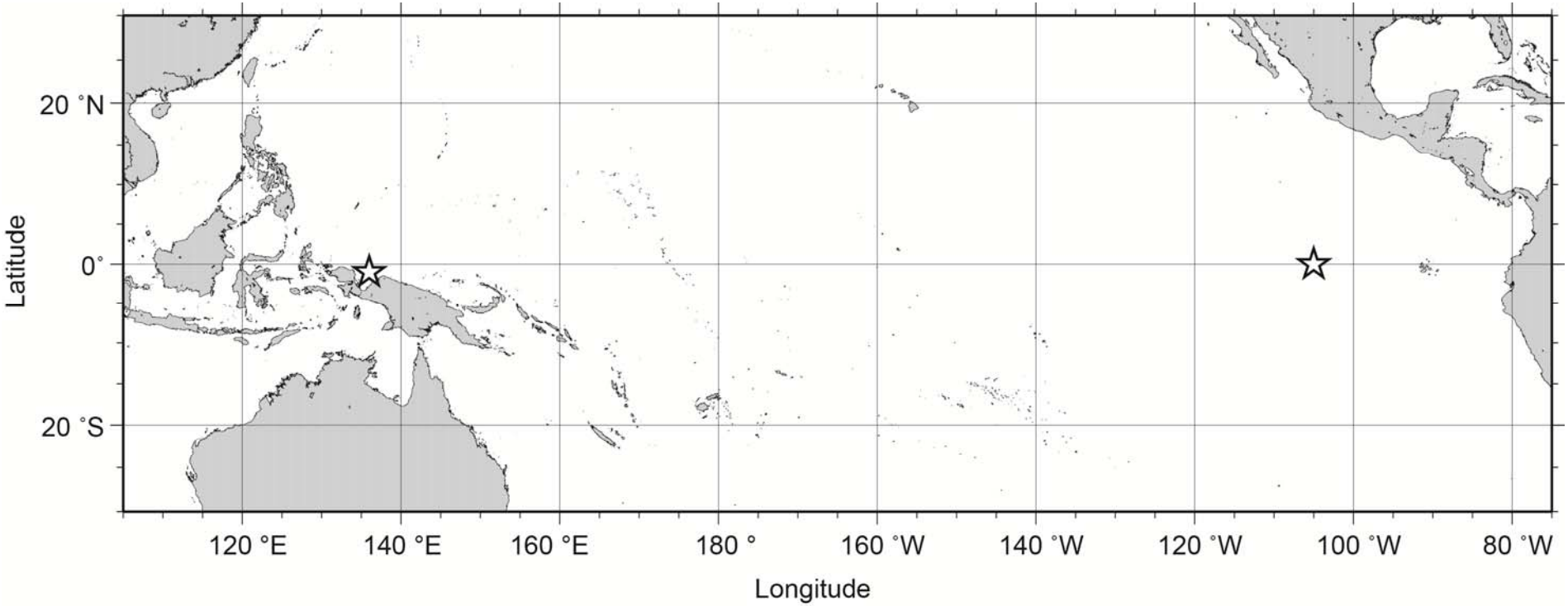
20 ˚N
0°
20 ˚S
Latitude
120 °E
140 °E
160 °E
180 °
160 ˚W
140 ˚W
120 ˚W
100 ˚W
80 ˚W
Longitude

Fig. 1

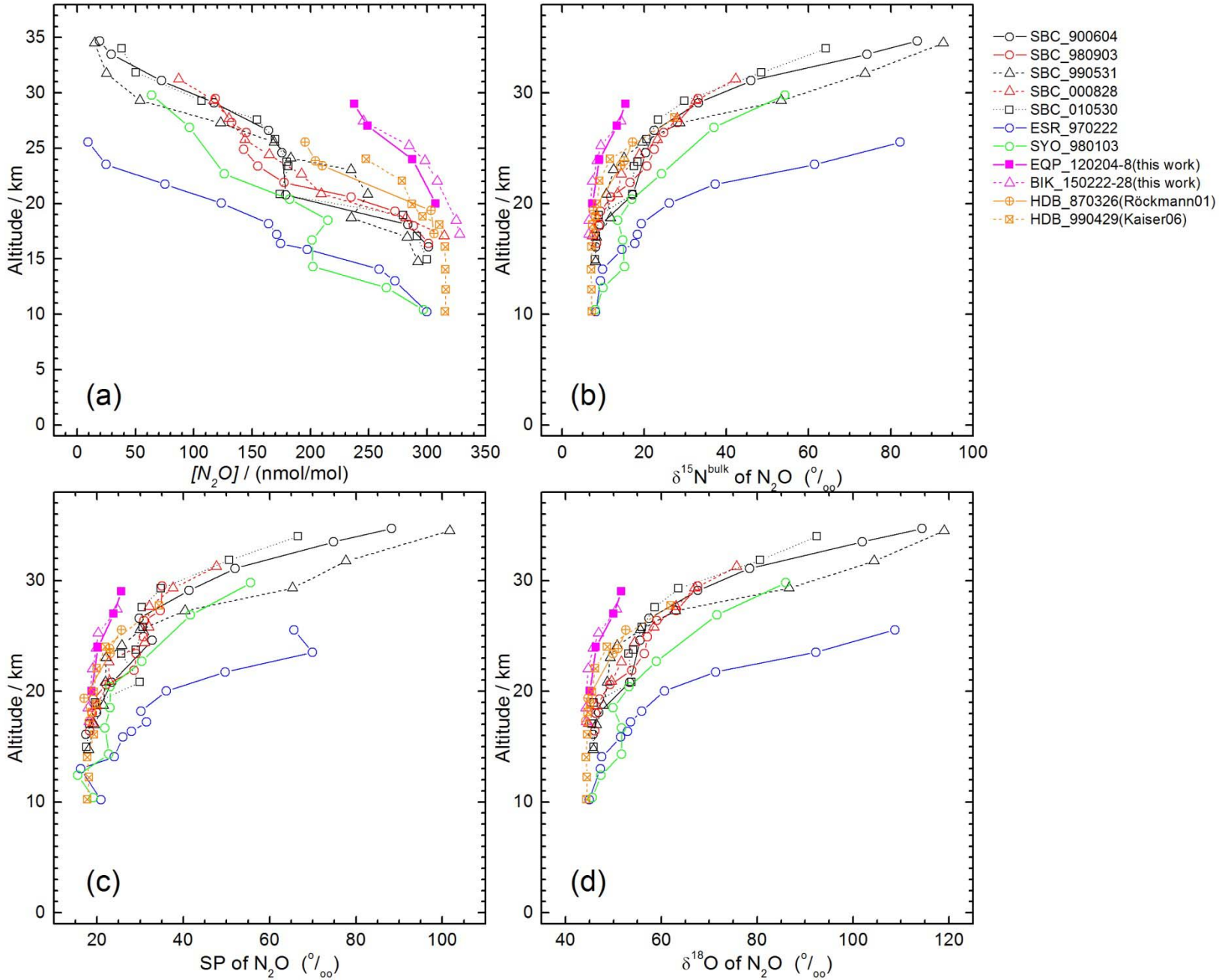
(a)
Altitude / km
[N2O] / (nmol/mol)
(b)
δ15Nbulk of N2O (°/oo)
(c)
SP of N2O (°/oo)
(d)
δ18O of N2O (°/oo)
SBC_900604
SBC_980903
SBC_990531
SBC_000828
SBC_010530
ESR_970222
SYO_980103
EQP_120204-8(this work)
BIK_150222-28(this work)
HDB_870326(Röckmann01)
HDB_990429(Kaiser06)

Fig. 2

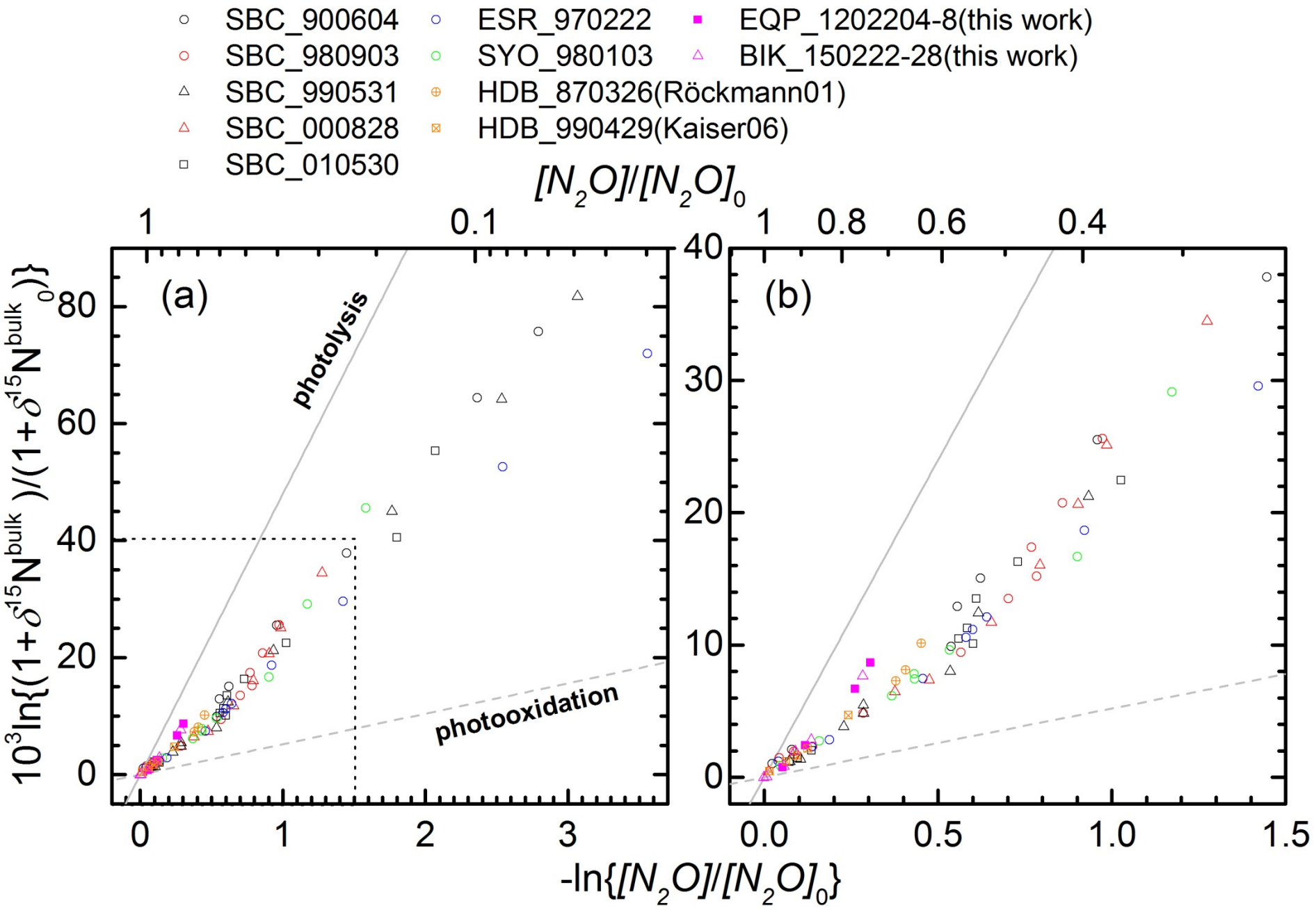
SBC_900604
SBC_980903
SBC_990531
SBC_000828
SBC_010530
ESR_970222
SYO_980103
HDB_870326(Röckmann01)
HDB_990429(Kaiser06)
EQP_1202204-8(this work)
BIK_150222-28(this work)
[N2O]/[N2O]0
(a)
(b)
photolysis
photooxidation
10^3 ln{(1+δ15N^bulk)/(1+δ15N^bulk_0)}
-ln{[N2O]/[N2O]0}

Fig. 3

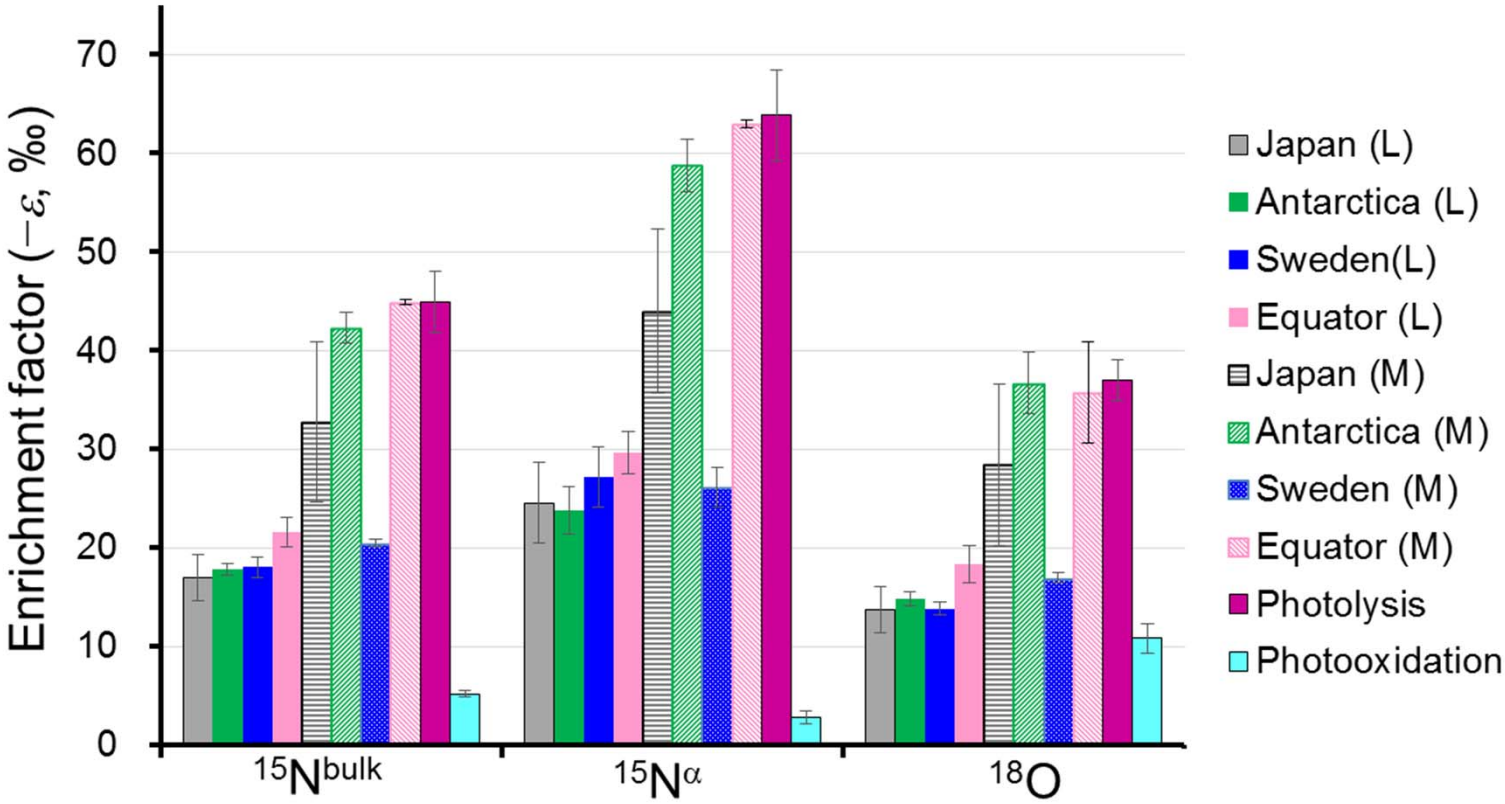
Enrichment factor (−ε, ‰)
70
60
50
40
30
20
10
0
15Nbulk
15Nα
18O
Japan (L)
Antarctica (L)
Sweden(L)
Equator (L)
Japan (M)
Antarctica (M)
Sweden (M)
Equator (M)
Photolysis
Photooxidation

Fig. 4

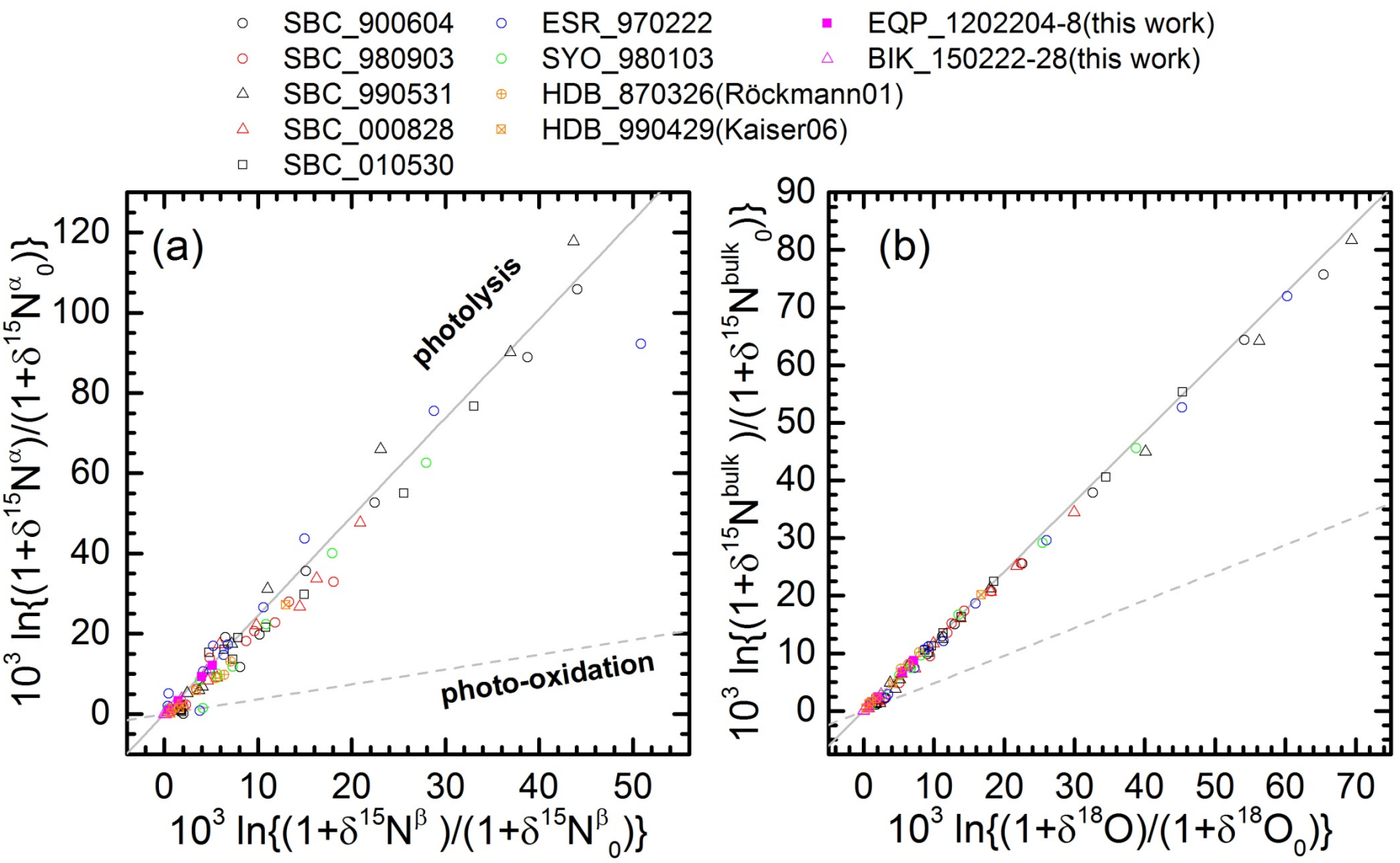
SBC_900604
SBC_980903
SBC_990531
SBC_000828
SBC_010530
ESR_970222
SYO_980103
HDB_870326(Röckmann01)
HDB_990429(Kaiser06)
EQP_1202204-8(this work)
BIK_150222-28(this work)
(a)
photolysis
photo-oxidation
$10^3 \ln\{(1+\delta^{15}N^{\alpha})/(1+\delta^{15}N^{\alpha}_0)\}$
$10^3 \ln\{(1+\delta^{15}N^{\beta})/(1+\delta^{15}N^{\beta}_0)\}$
(b)
$10^3 \ln\{(1+\delta^{15}N^{bulk})/(1+\delta^{15}N^{bulk}_0)\}$
$10^3 \ln\{(1+\delta^{18}O)/(1+\delta^{18}O_0)\}$

Fig. 5

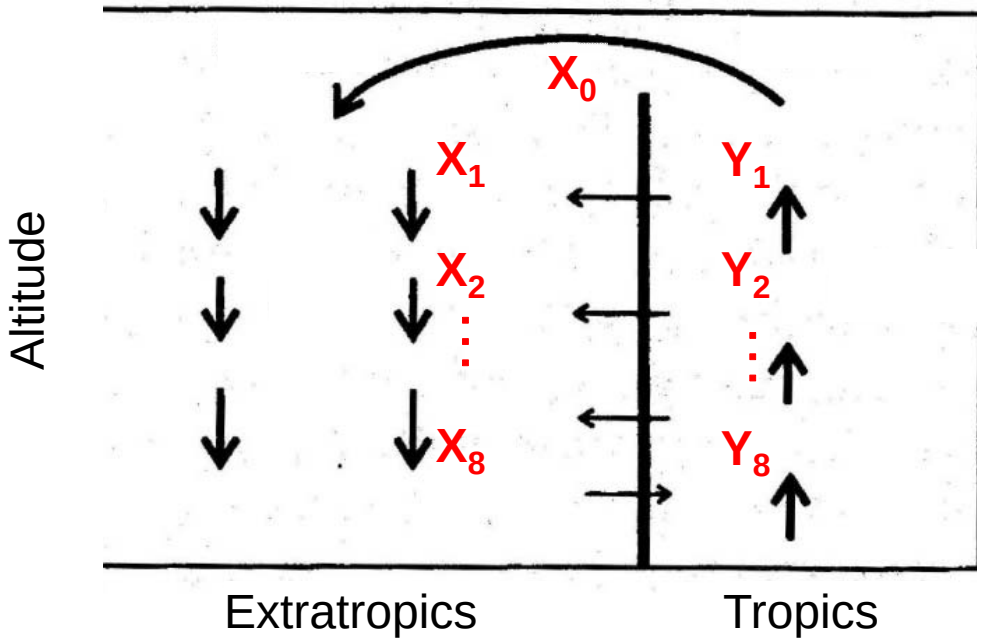

Fig. 6

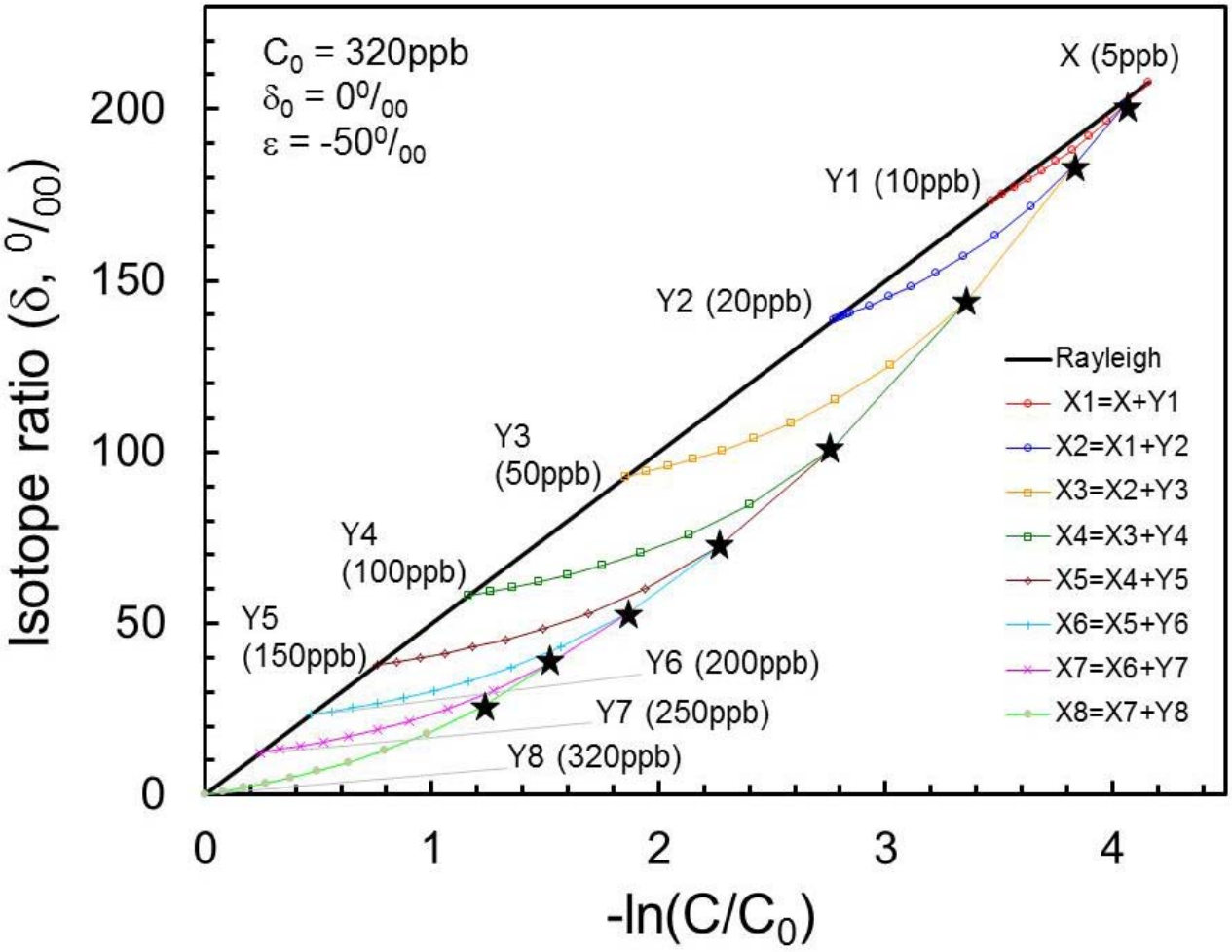
C0 = 320ppb
δ0 = 0‰
ε = -50‰
X (5ppb)
Y1 (10ppb)
Y2 (20ppb)
Y3
(50ppb)
Y4
(100ppb)
Y5
(150ppb)
Y6 (200ppb)
Y7 (250ppb)
Y8 (320ppb)
Rayleigh
X1=X+Y1
X2=X1+Y2
X3=X2+Y3
X4=X3+Y4
X5=X4+Y5
X6=X5+Y6
X7=X6+Y7
X8=X7+Y8
Isotope ratio (δ, ‰)
-ln(C/C0)
0
50
100
150
200
0
1
2
3
4

Fig. 7

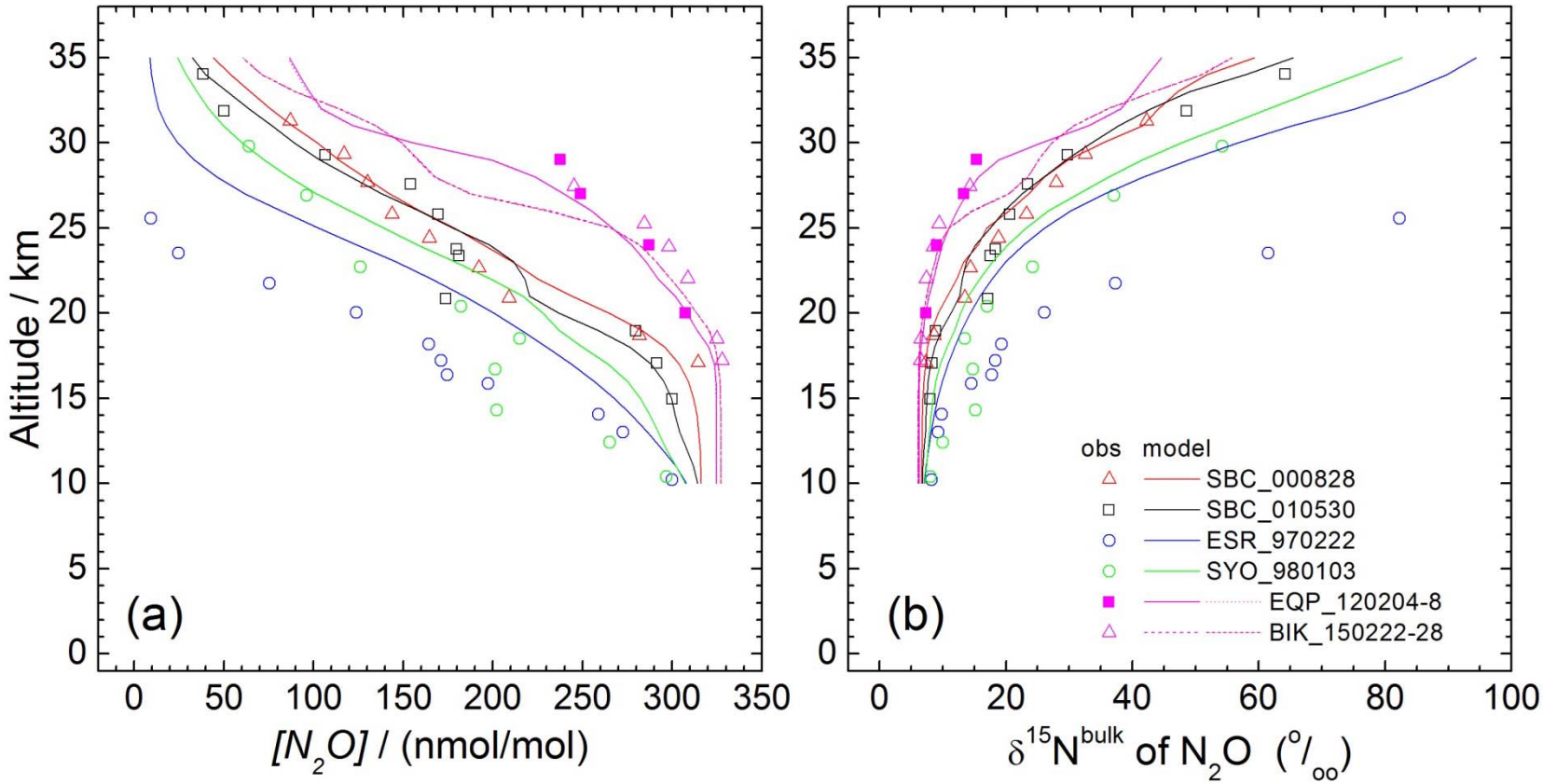
Altitude / km
[N2O] / (nmol/mol)
(a)
(b)
δ15Nbulk of N2O (o/oo)
obs model
SBC_000828
SBC_010530
ESR_970222
SYO_980103
EQP_120204-8
BIK_150222-28

Fig. 8

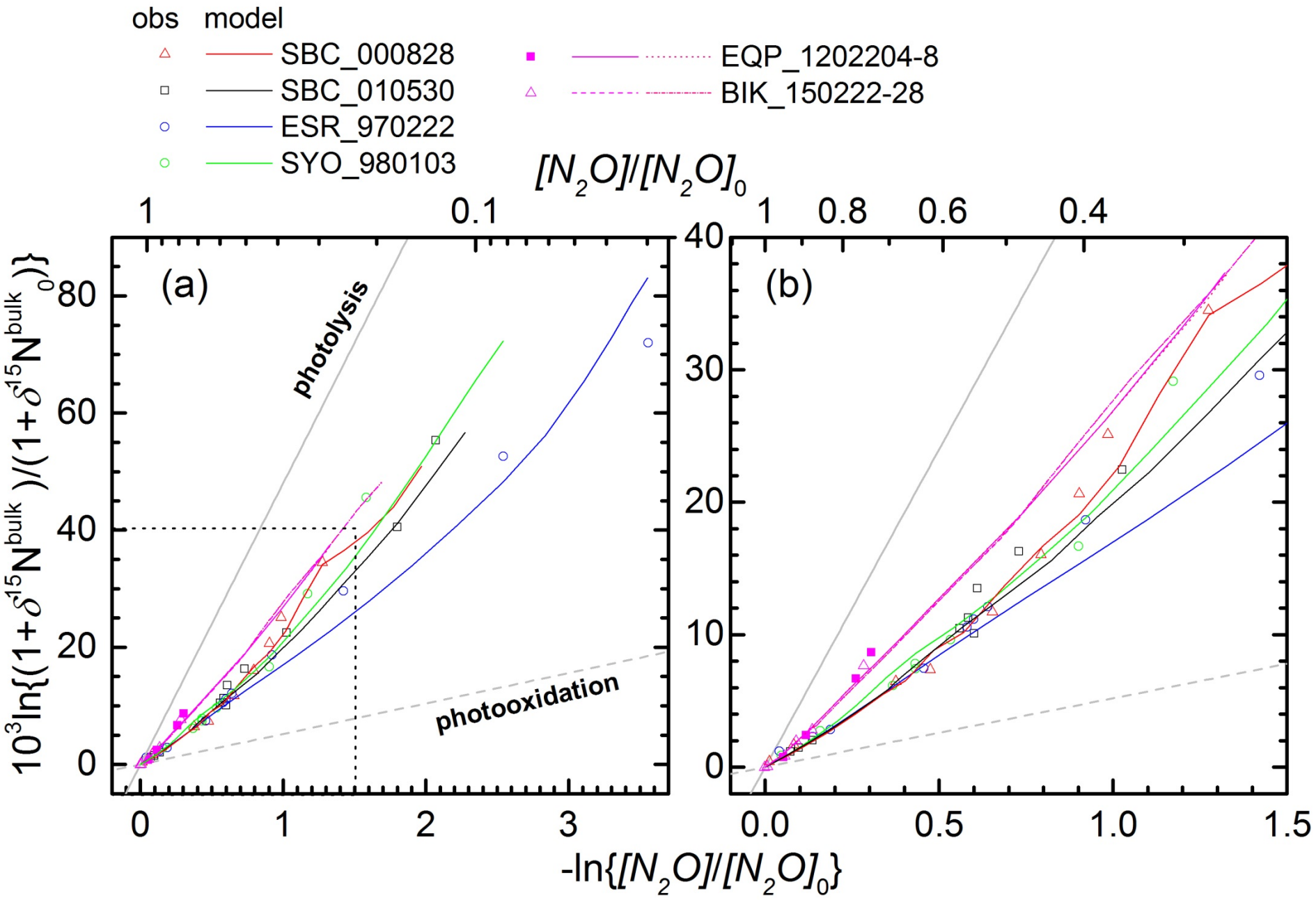
obs model
SBC_000828
SBC_010530
ESR_970222
SYO_980103
EQP_1202204-8
BIK_150222-28
[N2O]/[N2O]0
(a)
(b)
photolysis
photooxidation
10^3 ln{(1+δ15Nbulk)/(1+δ15Nbulk0)}
-ln{[N2O]/[N2O]0}

Fig. 9

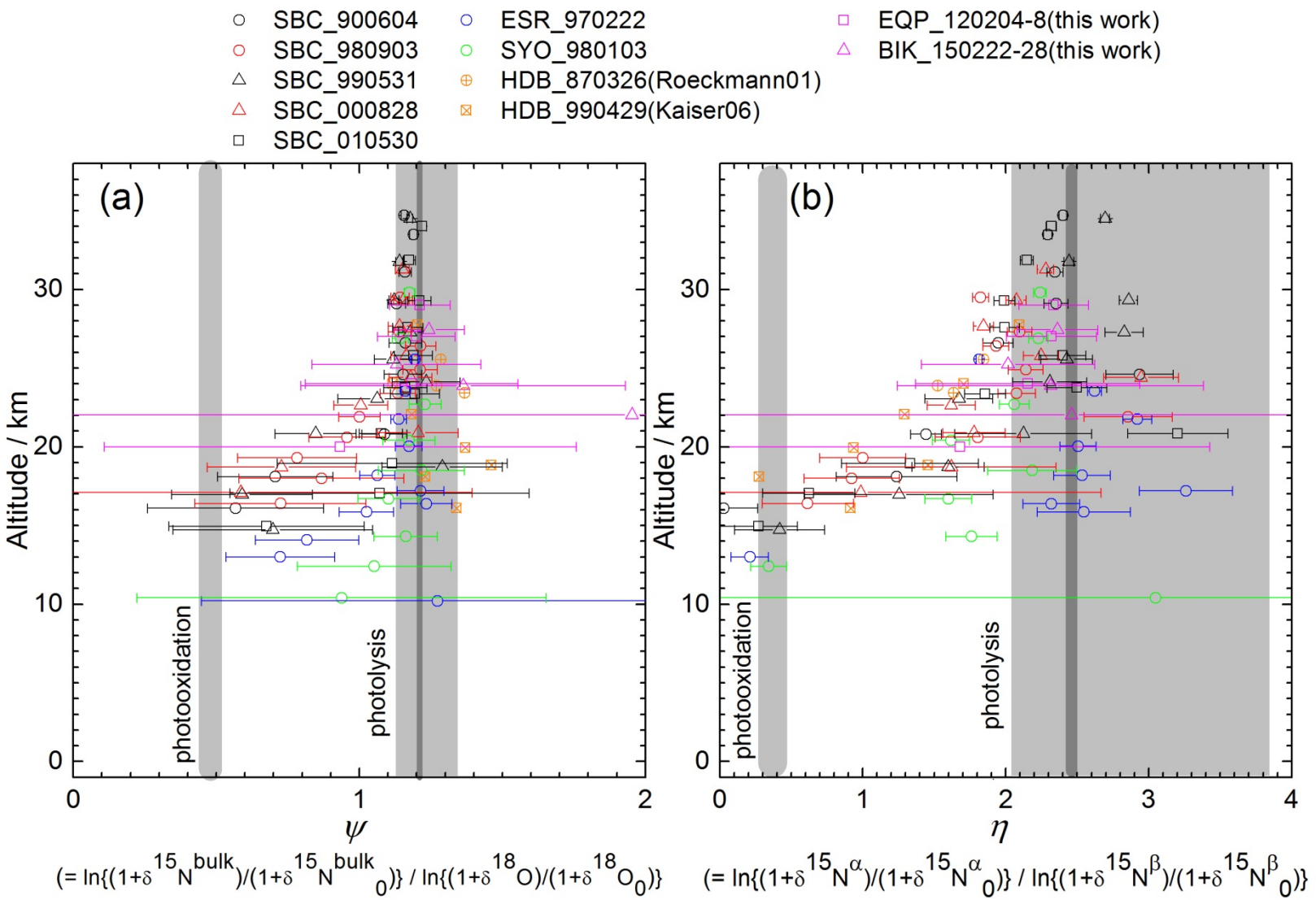
SBC_900604
SBC_980903
SBC_990531
SBC_000828
SBC_010530
ESR_970222
SYO_980103
HDB_870326(Roeckmann01)
HDB_990429(Kaiser06)
EQP_120204-8(this work)
BIK_150222-28(this work)
(a)
(b)
Altitude / km
photooxidation
photolysis
ψ
η
(= ln{(1+δ15Nbulk)/(1+δ15Nbulk0)} / ln{(1+δ18O)/(1+δ18O0)}
(= ln{(1+δ15Nα)/(1+δ15Nα0)} / ln{(1+δ15Nβ)/(1+δ15Nβ0)}

Fig. 10